Inorg. Chem. **2004**, *43*, 5529–5536

Inorganic Chemistry
Article

Synthesis of and Structural Studies on Lead(II) Cysteamin Complexes

Holger Fleischer*,† and Dieter Schollmeyer‡

Institut für Anorganische Chemie und Analytische Chemie and the Institut für Organische Chemie,
Universität Mainz, Duesbergweg 10 − 14, D-55099 Mainz, Germany

Received January 28, 2004

The novel compounds $PbCl_2 \cdot (SCH_2CH_2NH_3)$ (**1**), $Pb(SCH_2CH_2NH_2)_2 \cdot 2PbCl(SCH_2CH_2NH_2)$ (**2**), and $Pb(SCH_2CH_2NH_2)_2$ (**3**) were synthesized by reaction of PbO or $PbCl_2$ with $[HSCH_2CH_2NH_3]Cl$ and NaOH, and were characterized by elemental analysis, IR-, and UV/vis-spectroscopy. Single-crystal X-ray diffraction revealed different coordination modes for the two Pb atoms in **2**. The Pb atom in the $Pb(SCH_2CH_2NH_2)_2$ unit forms two covalent Pb–S and two intramolecular dative Pb···N bonds, leading to a pseudo trigonal bipyramidal configuration with a stereochemically active lone pair. The Pb atom in the $PbCl(SCH_2CH_2NH_2)$ unit, the first moiety structurally characterized of the PbCl(SR) type (R = organic group), forms covalent Pb–Cl and Pb–S bonds, an intramolecular dative Pb···N bond, and two intermolecular Pb···S contacts, giving a pseudo octahedral configuration with a stereochemically active lone pair as well. Despite the $Pb(SCH_2CH_2NH_2)_2$ moiety exhibiting C_2 symmetry in **2**, and C_1 symmetry in **3**, its structural parameters are rather similar in the two compounds. The influence of the Pb···N bond on molecular structure and thermodynamic stability were estimated by means of quantum chemical ab initio methods. Although an analysis of the wave function in terms of natural bond orbitals (NBO) revealed that n(N) and $n_p(S)$ compete for the empty p-orbital of the Pb^{II} atom, the σ-type n(N)–6p(Pb) interaction is stronger than the π-type $n_p(S)$–6p(Pb) interaction and hence determines the conformation of the compounds.

Introduction

Coordination of soft metal dications, M^{2+}, by peptides and proteins occurs preferably through S or N donor sites of amino acids, e.g., cysteine and histidine.[1] In that respect, Pb^{2+} and other thiophilic ions compete with Zn^{2+} for the coordination to cysteine in many protein sites,[2] and a part of the toxicity of lead is attributed to this feature. The ratio of Pb^{2+} to Zn^{2+} bound to a particular site was found to be determined by the relative affinities of the two metals to that site.[3] Compared to the vast amount of structurally characterized zinc thiolate complexes which serve as models of zinc-binding in enzymes,[4] only a few lead thiolate complexes with S,N coordination to Pb are known so far.[5,6,7] Some time ago, several 2-aminoethanethiolate complexes of bismuth(III) were synthesized and structurally characterized.[8] In a recent study, we investigated tellurium(II) thiolates derived from β-donor substituted thiols.[9] None of these compounds exhibits an intramolecular donor−acceptor interaction between the donor atom and the Te atom, a result attributed to a rigid CSTeS-conformation due to strong $n_p(S)$-$\sigma^*(Te-S)$ interactions. These results prompted us to study lead(II) complexes of donor-functionalized thiolates and to investigate the coordination geometry at the Pb atoms in these compounds. We here report the synthesis, IR investigations of all compounds depicted in Scheme 1 , and present UV/

---

* Author to whom correspondence should be addressed. E-mail: fleische@mail.uni-mainz.de. Fax: (+)49 6131 3925336.

† Institut für Anorganische Chemie und Analytische Chemie.

‡ Institut für Organische Chemie.

(1) Dance, I. G. *Polyhedron* **1986**, 5, 1037−1104.

(2) (a) Holm, R. H.; Kennepohn, P.; Solomon, E. I. *Chem. Rev.* **1996**, 96, 2239−2314. (b) Lipscomb, W. N.; Sträter, N. *Chem. Rev.* **1996**, *96*, 2375−2434.

(3) Payne, J. C.; ter Horst, M. A.; Godwin, H. A. *J. Am. Chem. Soc.* **1999**, *121*, 6850−6855, and references therein.

(4) See for example Makowska-Grzyska, M. M.; Jeppson, P. C.; Allred, R. A.; Arif, A. M.; Berreau, L. M. *Inorg. Chem.* **2002**, *41*, 4872−4887. Anjali, K. S.; Jeyagowry, T. S.; Vittal, J. J. *Inorg. Chim. Acta* **1999**, *295*, 9−17. Albrich, H.; Vahrenkamp, H. *Chem. Ber.* **1994**, *127*, 1223−1233. Jordan, K. J.; Wachtolz, W. F.; Crosby, G. A. *Inorg. Chem.* **1991**, *30*, 4588−4593. Casals, I.; González-Duarte, P.; López, C.; Solans, X. *Polyhedron* **1990**, *9*, 763−768. Corwin, D. T., Jr.; Koch, S. A. *Inorg. Chem.* **1988**, *27*, 493−496. Bell, P.; Sheldrick, W. S. *Z. Naturforsch.* **1984**, *39b*, 1732−1737.

(5) Agre, V. M.; Shugam, E. A. *Zh. Strukt. Khim. (Russ.) (Russ. J. Struct. Chem.)* **1971**, *12*, 102−107.

(6) Pech, L. Y.; Ozols, Y., K.; Apinitis, S. K.; Sturis, A. P. *Latv. PSR Zinat. Akad. Vestis, Khim. Ser.* **1982**, 26−27.

(7) Pech, L.; Bankovsky, Y.; Fundamensky, V.; Sturis, A.; Bruvere, A. *Latv. Khim. Z. (Latvian J. Chem.)* **1992**, 488−493.

(8) Briand, G. G.; Burford, N.; Cameron, T. S.; Kwiatkowski, W. *J. Am. Chem. Soc.* **1998**, *120*, 11374−11379.

(9) Fleischer, H.; Schollmeyer, D. *Inorg. Chem.* **2002**, *41*, 4739−4747.

10.1021/ic0498889 CCC: $27.50 © 2004 American Chemical Society
Published on Web 08/03/2004

Scheme 1. Structural Formulas of Compounds **1**−**3**

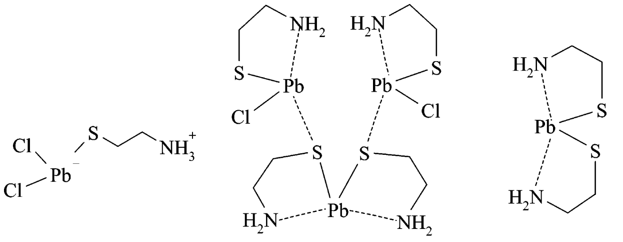

vis spectroscopic results and experimental and ab initio quantum chemical studies on the structures of $Pb(SCH_2CH_2NH_2)_2 \cdot 2PbCl(SCH_2CH_2NH_2)$ and of $Pb(SCH_2CH_2NH_2)_2$.

Results and Discussion

Synthesis. Complex **1** was obtained by reaction of $PbCl_2$ with $[HSCH_2CH_2NH_3]Cl$ and NaOH in a ratio 1:2:2. Elemental analysis suggests **1** to be a 1:1 adduct between $PbCl_2$ and $SCH_2CH_2NH_3$, analogous to the reaction of $BiCl_3$ with $SCH_2CH_2NH_3$.[8,10,11] Presumably, $SCH_2CH_2NH_3$ is formed from $[HSCH_2CH_2NH_3]Cl$ and NaOH first and then adds to $PbCl_2$, according to reaction 1

$$PbCl_2 + [HSCH_2CH_2NH_3]Cl + NaOH \rightarrow \mathbf{1} + NaCl + H_2O \quad (1)$$

Obviously, the reaction did not proceed further, neither by addition of a second $SCH_2CH_2NH_3$ ligand to the Pb^{II} center nor via elimination of HCl toward formation of $PbCl(SCH_2CH_2NH_2)$. Change of the $PbCl_2/[HSCH_2CH_2NH_3]Cl/NaOH$ ratio to 1:2:5 or even 1:2:7, led to the formation of the trinuclear lead complex **2**, according to reaction 2

$$3\ PbCl_2 + 4\ [HSCH_2CH_2NH_3]Cl + 8\ NaOH \rightarrow \mathbf{2} + 8\ NaCl + 8\ H_2O \quad (2)$$

The excess of NaOH leads to deprotonation of the $-NH_3$ group and subsequently allows formation of intramolecular Pb···N interactions. It is surprising that complex **2** does not react with the thiolate anions still present in the solution, since Pb^{II} is known to be a soft Lewis acid that preferentially binds to S-donor ligands. A similar observation was made in course of the synthesis of $Bi(SCH_2CH_2NH_2)_3$.[8] This compound could not be obtained from a stoichiometric reaction of $BiCl_3$ and $KSCH_2CH_2NH_2$ but afforded a large excess of the anionic ligand. We succeeded with the synthesis of **3** by using PbO together with 2.5 equiv of $[HSCH_2CH_2NH_3]Cl$ and NaOH each, according to reaction 3

$$PbO + 2\ [HSCH_2CH_2NH_3]Cl + 2\ NaOH \rightarrow \mathbf{3} + 2\ NaCl + 3\ H_2O \quad (3)$$

In contrast to the synthesis of **1**, the reaction does not terminate after formation of $SCH_2CH_2NH_3$ and its addition to Pb^{II}, but proceeds via cleavage of the Pb−O bonds. In the synthesis of **2**, a stoichiometric excess of thiolate ions was not sufficient to shift the equilibrium (reaction 4) toward the right side. On the other hand, compound **3** could be synthesized in the presence of Cl^- ions (see reaction 3). Hence concerning the equilibrium (4)

$$\mathbf{2} + 2\ (SCH_2CH_2NH_2)\text{-} \rightleftharpoons 3\ \mathbf{3} + 2\ Cl^- \quad (4)$$

it follows that either complex **2** or **3** (or both) must be kinetically stabilized.

Spectroscopy. Assignment of vibrational modes of compounds **1**−**3** was achieved using scaled (scale factor 0.95) MP2/LANL2DZ(d) calculated vibrational frequencies. According to these calculations, ν(Pb−S) and ν(Pb−Cl) are below 200 cm^{-1} and hence fall outside the IR spectral range. Any attempt to record Raman spectra of **1**−**3** to observe these bands failed due to the strong fluorescence of the compounds while irradiated at $\lambda = 1064$ nm. As well, no useful information was obtained when ^{207}Pb NMR spectra of the compounds **1**−**3** were recorded, either in aqueous solution or in the solid state. In solution, no signal could be detected, and in the solid state, even at spinning rates of 15 kHz, only very broad signals occurred. IR results neither contradict nor support the coordination mode at the Pb atom in **1**, and its structural formula presented in Scheme 1 is to be seen as a suggestion.

Complexes **2** and **3** are colorless, in contrast to **1** which is a yellow compound. The UV spectra of **2** ($c = 1.23\ 10^{-5}$ M) and **3** ($c = 4.00\ 10^{-5}$ M) in aqueous solution both display a band around 201−202 nm which is attributed to the free Pb^{2+} ion.[12] Obviously, the complexes dissociate at least partially at these low concentrations. An additional peak around 270 nm which occurs in both spectra might be due to a $[Pb(SCH_2CH_2NH_2)]^+$, $Pb(SCH_2CH_2NH_2)2$, or a hydroxo complex containing the $Pb(SCH_2CH_2NH_2)$ fragment. Bands due to the cysteamine ligand were not observed,[13] probably due to its covering by the band of the Pb^{2+} ion.

Crystal and Molecular Structure of 2. The crystal structure of **2** consists of chains of $PbCl(SCH_2CH_2NH_2)$ (**2a**) running along the *b*-axis, in which the molecules are held together via intermolecular Pb···S bonds. In one direction, these chains are linked by $Pb(SCH_2CH_2NH_2)_2$ (**2b**) in such a way that each molecule of **2b** forms Pb···S contacts and N−H···Cl hydrogen bridges to two molecules of **2a** situated in different chains (see Figure 1b). In the other direction, there are N−H···Cl hydrogen bridges between those chains. A Pb−S···Pb−S chain structure was also recently reported by Jurkschat and co-workers for the compound 4-*t*Bu-2,6-$[P(O)(OEt)_2]_2C_6H_2PbSPh$.[14] In the latter, the covalent Pb−S distance is similar to that in **2a**, while its Pb···S distance is significantly larger. Molecules of **2b** lay on special positions and exhibit C_2-symmetry. The $SCH_2CH_2NH_2$-ligand acts in **2a** and in **2b** in a chelating, bidentate S,N-coordination mode.

---

[10] Briand, G. G.; Burford, N.; Cameron, T. S. *Chem. Commun.* **1997**, 2365−2366.

[11] In aqueous solution and in the solid state, cysteamin is present as the zwitterionic $SCH_2CH_2NH_3$ tautomer. Fleischer, H.; Schollmeyer, D. manuscript submitted for publication.

[12] (a) Fromherz, H.; Lih, K. H. *Z. Physik. Chem.* **1931**, *153A*, 321−375. (b) Hagemann, S. PhD thesis, Brauschweig, Germany, **1998**.

[13] De Deken, R. H.; Broekhuysen, J.; Bechet, J.; Mortier, A. *Biochim. Biophys. Acta* **1956**, *19*, 45−52.

[14] Jurkschat, K.; Peveling, K.; Schürmann, M. *Eur. J. Inorg. Chem.* **2003**, 3563−3571.

Table 1. Selected Structural Data of **2** from Single Crystal XRD (Distances in Å, Angles in deg)[a,b]

			2a		
Pb1A−S1A	2.696(2)	S1A-Pb1A-Cl1A	92.3(1)	Cl1A-Pb1A−S1A−C2A	−83.4(2)
Pb1A-Cl1A	2.791(2)	S1A-Pb1A−N4A	76.3(1)	Pb1A−S1A−C2A−C3A	33.8(5)
Pb1A−N4A	2.409(5)	S1A-Pb1A−S1A#1	89.6(1)	S1A−C2A−C3A−N4A	−61.0(6)
Pb1A−S1A#1	3.036(2)	S1A-Pb1A−S1B	69.4(1)	C2A−C3A−N4A-Pb1A	55.9(5)
Pb1A−S1B	3.285(2)	N4A-Pb1A−S1B	145.7(1)	S1A-Pb1A−N4A−C3A	−25.8(4)
S1A−C2A	1.842(6)	Cl1A-Pb1A−S1A#1	168.1(1)	N4A-Pb1A−S1A−C2A	−4.0(2)
C2A−C3A	1.508(8)	Pb1A−S1A-Pb1A#2	105.8(1)	S1A#1-Pb1A−S1A-Pb1A#2	−4.94(2)
C3A−N4A	1.477(7)	C3A−N4A-Pb1A	113.4(3)		
			2b		
Pb1B−N4B	2.592(6)	S1B−Pb1B−S1B#3	93.5(1)	S1B#3-Pb1B−S1B−C2B	−68.8(2)
Pb1B−S1B	2.635(2)	N4B−Pb1B−N4B#3	149.9(2)	Pb1B−S1B−C2B−C3B	−45.6(5)
S1B−C2B	1.822(8)	S−Pb−S/N−Pb−N[c]	84.9	S1B−C2B−C3B−N4B	66.8(7)
C2B−C3B	1.502(10)	C3B−N4B−Pb1B	110.3(4)	C2B−C3B−N4B−Pb1B	−47.8(6)
C3B−N4B	1.478(9)			S1B−Pb1B−N4B−C3B	15.4(4)
				N4B−Pb1B−S1B−C2B	13.5(3)
			Hydrogen Bridges		
N4A···Cl1A#4	3.403(5)	N4A−H4A···Cl1A#4	143.7		
N4A···S1B#5	3.398(6)	N4A−H4B···S1B#5	174.8		
N4B···Cl1A#6	3.421(6)	N4B−H4C···Cl1A#6	152.2		
N4B···Cl1A#7	3.571(6)	N4B−H4D···Cl1A#7	138.2		

[a] See text for the definition of **2a** and **2b**. [b] Symmetry transformations used to generate equivalent atoms: #1 $-x + 1.5$, $y + 0.5$, $-z + 1.5$; #2 $-x + 1.5$, $y - 0.5$, $-z + 1.5$; #3 $-x$, y, $-z + 1.5$; #4 $-x + 1.5$, $-y - 0.5$, $-z + 2$; #5 $x + 1$, $y - 1$, z; #6 $x - 0.5$, $y + 0.5$, z; #7 $x - 0.5$, $y + 1.5$, z. [c] S−Pb−S/N−Pb−N defines the angle between the S1B−Pb1B−S1B#3 and the N4B−Pb1B−N4B#3 plane.

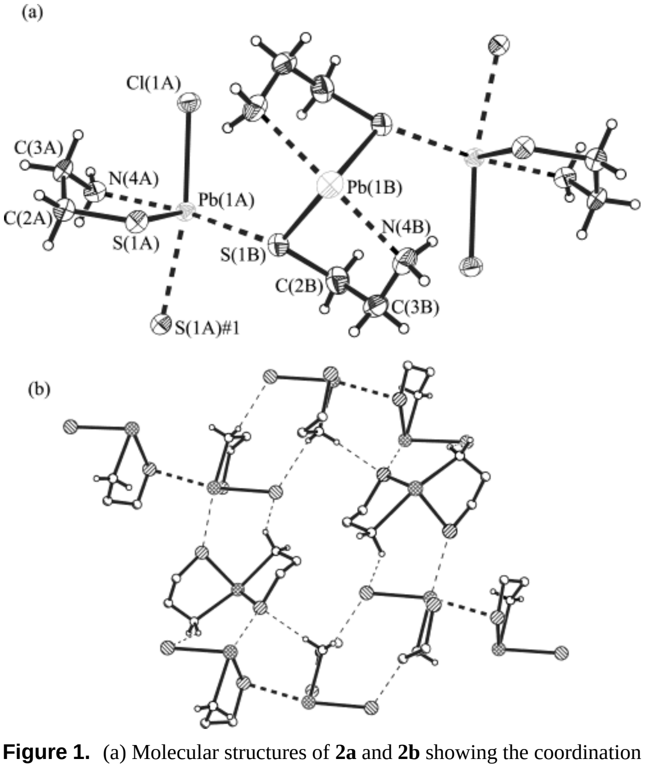

Figure 1. (a) Molecular structures of **2a** and **2b** showing the coordination modes of the Pb atoms. Displacement ellipsoids are at the 50% probability level. (b) Packing of **2** showing the N−H···S and N−H···Cl hydrogen bridges. Hydrogen atoms bound to carbon atoms are omitted for clarity.

$PbCl(SCH_2CH_2NH_2)$ is the first moiety structurally characterized of the PbCl(SR) type (R = organic group). Pb1A (**2a**) is coordinated by S1A and Cl1A (covalent bonds), N4A (intramolecular dative bond), S1A#, and S1B (intermolecular dative bonds), giving a coordination number of five.[15] **2** is the first example for a compound containing a Pb atom with a $Pb(S_3NCl)$ coordination mode. Since the lone pair at Pb1A is stereochemically active, the atom exhibits a distorted pseudo-octahedral configuration (see Figure 1a). For Pb1A, calculation of the valence bond orders according to O'Keeffe and Brese gave the following values: 0.643 for Pb1A−S1A, 0.257 for Pb1A−S1A#1, 0.131 for Pb1A−S1B, 0.420 for Pb1A−Cl1A, and 0.591 for Pb1A−N4A, giving a bond valence sum of 2.042, in good accordance with the ideal value of 2 for Pb^{II}.[16] The five-membered chelating ring at Pb1A adopts an envelope conformation with C3A being by 0.663 Å out of the least-squares plane through the other four atoms. Pb1B does not form intermolecular contacts and is coordinated by two S atoms (covalent bonds) and two N atoms (dative bonds), giving a coordination number of four and a slightly distorted pseudo trigonal bipyramidal configuration. The N atoms occupy the apical positions and are tilted away from the lone pair (see Figure 1a). The angle between the S−Pb−S and the N−Pb−N planes is close to 90°. Such a $Pb(S_2N_2)$ coordination mode was already observed for several 8-mercaptoquinolinato derivatives of Pb^{II}.[5−7] The following valence bond orders for Pb1B were obtained: 0.758 for Pb1B−S1B and 0.360 for Pb1B−N4B. Since two of each bonds are present in **2b**, a bond valence sum of 2.236 results, indicating the presence of a hypervalent Pb^{II}. The five-membered chelating ring at Pb1B adopts a twist conformation with C2B and C3B being by 0.421 and 0.367 Å above and below the S1A-Pb1A−N4A plane, respectively. Pb1A−N4A represents a two-center−two-electron dative bond and the respective Pb−N distance is much shorter than those in the three-center−four-electron bond N4B−Pb1B−N4B#3 in **2b** (see Table 1). All in all, the structure of **2** shows some similarities to that of $Pb(SAr)_2$ (Ar = 2,6-diisopropylphenyl),[17] where trimeric C_2-symmetric $[Pb(SAr)_2]_3$ units are present. The distance between Pb1A

---

(15) Covalent and dative bonds are distinguished according to the definition by Haaland: Haaland, A. *Angew. Chem.* **1989**, *101*, 1017−1032. Haaland, A. *Angew. Chem. Int. Ed. Engl.* **1989**, *28*, 992−1007.

(16) O'Keeffe, M.; Brese, N. E. *J. Am. Chem. Soc.* **1991**, *113*, 3226−3229.

(17) Hitchcock, P. B.; Lappert, M. F.; Samways, B. J.; Weinberg, E. L. *Chem. Commun.* **1983**, 1492−1494.

Table 2. Selected Structural Data of **3** from Single Crystal XRD (Distances in Å, Angles in deg)[a]

Pb1−S5	2.633(3)	S5−Pb1−S1	99.2(1)	S5−C6−C7−N8	−62.6(14)
Pb1−S1	2.639(3)	N4−Pb1−N8	149.3(3)	C2−C3−N4−Pb1	53.7(11)
Pb1−N4	2.550(8)	S−Pb−S/N−Pb−N[b]	83.8	C6−C7−N8−Pb1	44.2(11)
Pb1−N8	2.626(9)	C3−N4−Pb1	109.4(7)	C3−N4−Pb1−S1	−24.7(6)
S1−C2	1.820(12)	C7−N8−Pb1	109.8(7)	C7−N8−Pb1−S5	−14.4(7)
C2−C3	1.481(15)	S5−Pb1−S1−C2	75.1(4)	N4−Pb1−S1−C2	−3.2(5)
C3−N4	1.472(13)	S1−Pb1−S5−C6	74.3(4)	N8−Pb1−S5−C6	−11.3(5)
S5−C6	1.798(13)	Pb1−S1−C2−C3	32.8(10)		
C6−C7	1.445(15)	Pb1−S5−C6−C7	43.2(11)		
C7−N8	1.529(16)	S1−C2−C3−N4	−61.1(13)		
		Hydrogen Bridges			
N4···S5#1	3.498(9)	N4−H4A···S6#1	156.2		
N4···S5#2	3.501(9)	N4−H4B···S6#2	155.0		
N8···S1#3	3.615(10)	N8−H8A···S1#3	148.7		
N8···S1#4	3.587(9)	N8−H8B···S1#4	163.1		

[a] Symmetry transformations used to generate equivalent atoms: #1 $-x+1, -y+1, -z+1$; #2 $-x+0.5, -y+1, z+0.5$; #3 $x, -y+0.5, z-0.5$; #4 $x-0.5, y, -z+0.5$ [b] S−Pb−S/N−Pb−N defines the angle between the S1−Pb1−S5 and the N4−Pb1−N8 plane.

Table 3. Selected Structural Parameters (Internuclear Distances in Å, Bonding and Torsion Angles in deg) of Several Tetra Coordinate Lead(II) Compounds Exhibiting a $Pb(S_2N_2)$ Coordination Mode

	Pb−S$_{av}$	Pb−N$_{av}$	S−Pb−S	N−Pb−N	reference
2b	2.635(2)	2.592(6)	93.5(1)	149.9(2)	this work
3	2.636(3)	2.593(9)	99.2(1)	149.3(3)	this work
$Pb(C_9H_6NS)_2$[a]	2.715	2.481	99.1	137.2	5
$Pb(C_{12}H_{12}NS)_2$[b]	2.626(12)	2.642(13)	93.1	139.9	6
$Pb(C_{10}H_8NS_2)_2$[c]	2.635(4)	2.587(10)	93.9	143.6	7
$Pb(3\text{-}CF_3\text{-}pyS)_2$	2.795(11)	2.69(3)	86.4(3)	129.0(10)	19
$Pb(SSi(O^tBu)_3)_2(1,10\text{-phen})$	2.661	2.740	88.3	60.7	20

[a] Lead bis(8-mercapto-quinolinolate). [b] Lead bis(2-isopropyl-8-mercaptoquinolinate). [c] Lead bis(2-mkethylthio-8-mercaptoquinolinate).

and Pb1B amounts to 4.293 Å and is bigger than two times the van der Waals radii of Pb. Furthermore, the mutual orientation of **2a** and **2b** is such that the two Pb atoms cannot favorably interact with each other. Such Pb···Pb interactions were observed in some plumbylenes such as $Pb(mes)_2$, which is hence also described as $Pb_2(mes)_4$.[18]

Crystal and Molecular Structure of 3. The molecules of **3** and **2b** exhibit the same composition, and in both the Pb atom exhibits the same coordination mode (Figure 2). As with **2**, no intermolecular Pb···Pb-contacts are present in **3**. Comparison of **3** and **2b** allows study of the impact of different environments on structural parameters of the same molecule. Due to lattice symmetry **2b** exhibits molecular C_2-symmetry, whereas **3** lacks any molecular symmetry elements. The two Pb−N distances of the three-center−four-electron bond of **3** are markedly different, while the two Pb−S bonds are of similar length (Table 2). On the other side, the average Pb−S and Pb−N distances and the N−Pb−N angle of **3** and the corresponding values of **2b** do not differ significantly, and the bond valence sum of 2.245 for Pb1 is very similar to that of Pb1B in **2b** (vide infra). Hence, the weak Pb−N bonds are much more sensitive to changes in the molecular environment than the stong covalent Pb−S bonds.

A few Pb complexes exhibiting $Pb(S_2N_2)$ coordination are known (see Table 3). Pb−N bonds are shorter and Pb−S bonds are longer in lead bis(8-mercapto-quinolinolate) than in **2b** and **3**, suggesting a stronger donor power of the 8-mercaptoquinolinate N-atom compared to the primary amine group in 2-aminoethanethiole. The bulky substituents adjacent to the N-atom in lead bis(2-isopropyl-8-mercaptoquinolinate) and in lead bis(2-methylthio-8-mercaptoquinolinate) compensate this effect and lead to Pb···N and Pb−S bonds of a lengths similar to those found in **2b** and **3**. $Pb(3\text{-}CF_3\text{-}pyS)_2$ and $Pb(SSi(O^tBu)_3(1,10\text{-phen})$ also exhibit tetra coordinate Pb^{II} atoms with a $Pb(S_2N_2)$ coordination mode. The structure of $Pb(3\text{-}CF_3\text{-}pyS)_2$ consists of discrete molecules and with the lead atom coordinated by two bidentate (N,S) anionic 3-(trifluoromethyl)pyridine-2-thionato ligands. The environment around the lead atom is best described as

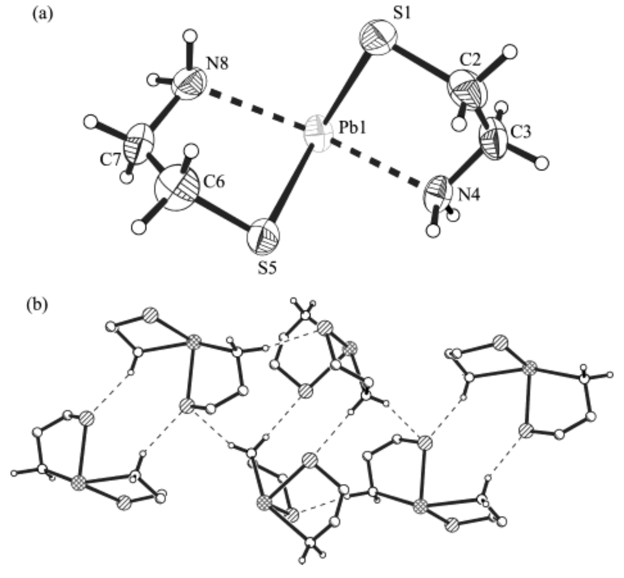

Figure 2. (a) Molecular structure of **3**. Displacement ellipsoids are at the 50% probability level. (b) Packing of **3** showing the N−H···S hydrogen bridges. Hydrogen atoms bound to carbon atoms are omitted for clarity.

---

(18) Stürmann, M.; Saak, W.; Weidenbruch, M.; Klinkhammer, K. W. *Eur. J. Inorg. Chem.* **1999**, 579−582.

Table 4. Selected ab Initio Structural Parameters (internuclear distances in Å, Bonding and Torsion Angles in deg) and Thermochemical Data (in kJ·mol^{-1}) of $PbCl(SCH_2CH_2NH_2)$ (C_1-symmetry) With (**IIa**) and Without (**IIb**) Intramolecular Pb−N Bond and of $Pb(SCH_2CH_2NH_2)_2$ (C_2-symmetry) With (**IIIa**) and Without (**IIIb**) Intramolecular Pb−N Bond (see Figure 3)

	IIa	IIIa
Pb1−S1	2.566	2.599
Pb1−Cl5	2.520	
Pb1···N4	2.429	2.624
S1−Pb1−X[c]	101.8	96.2
S1−Pb1···N4	79.4	76.2
Cl5−Pb1···N4	79.5	
X-Pb1−S1−C2	76.1	−53.8
Pb1−S1−C2−C3	−28.6	−54.9
S1−C2−C3−N4	59.4	65.0
E[n(N)−6p(Pb)][a]		232.8
q(Pb)/*q*(S)/*q*(N)[b]	+1.23/−0.51/−1.01	+1.13/−0.54/−0.98
q(Cl)[b]	−0.71	

	IIb	IIIb
Pb1−S1	2.488	2.495
Pb1−Cl5	2.441	
S1−Pb1−X[c]	96.6	94.6
X-Pb1−S1−C2[c]	177.0	175.7
Pb1−S1−C2−C3	−91.6	−101.0
S1−C2−C3−N4	−174.5	−178.3
E[n_p(S)−6p(Pb)][a]		206.0
q(Pb)/*q*(S)/*q*(N)[b]	+1.20/−0.51/−0.92	+1.07/−0.47/−0.93
q(Cl)[b]	−0.68	
Δ*E* [d]	−79.0	−121.7

[a] Energy of the respective orbital interaction per molecule due to an NBO analysis (see text). 6p(Pb) denotes the empty valence p-orbital of the Pb atom. [b] Natural atomic charges in elemental units. [c] X = S5 for $Pb(SCH_2CH_2NH_2)_2$ and X = Cl5 for $PbCl(SCH_2CH_2NH_2)$. [d] Δ*E* = *E*(with Pb−N bond) − *E*(without Pb−N bond).

a strongly distorted pseudo-trigonal bipyramid with the nitrogen atoms in axial and the sulfur atoms and the lone pair in equatorial positions. $Pb(SSi(O^tBu)_3(1,10\text{-phen})$ exhibits a configuration different from those of the other complexes presented in Table 3. Due to steric restrictions of the phenanthroline ring system, the N−Pb−N angle is much more narrow than in the other cases. As a consequence, one N atom sits in an equatorial position of the pseudo trigonal bipyramid and is much closer to the Pb center than the N atom which occupies the apical site.

Ab Initio Geometry Optimization, Thermochemical Calculations, and Investigation of the Intramolecular Pb−N Bond. The molecular structures of $PbCl(SCH_2CH_2NH_2)$ (conformers **IIa** and **IIb**) and $Pb(SCH_2CH_2NH_2)_2$ (conformers **IIIa** and **IIIb**; see Table 4 and Figure 3) were investigated by means of ab initio geometry optimization to estimate the stabilization energy gained by the Pb−N interaction and to study its influence on other structural parameters.[21] The results reveal that the presence of an intramolecular Pb−N bond significantly stabilizes the compound (see Table 4). Since **IIIa** exhibits two such Pb−N interactions, forming a three-center−four-electron (3c4e) bond, its stabilization relative to **IIIb** is bigger than the stabilization of **IIa**, where only a two-center−two-electron (2c2e) Pb−N bond is present, relative to **IIb**. As would be expected, the stabilization energy of **IIIa** is less than twice the stabilization energy of **IIa** (see also further down). The Pb−S and Pb−Cl bonds are substantially lengthened by the presence of the Pb−N bonds. This is despite the fact that the lone pair of the N atom mainly interacts with the empty p-orbital of the Pb atom and energies of interaction with σ^*(Pb−S) or σ^*(Pb−Cl) are rather small, i.e., less than 8 kJ·mol^{-1} for **IIa** and less than 24 kJ·mol^{-1} for **IIIa**, compared to 232.8 kJ·mol^{-1} for the n(N)−6p(Pb) interactions in **IIIa** (analysis in terms of natural bond orbitals, NBO, see also Table 4[22]). Changes in atomic charges with formation of the dative Pb−N bond are as expected, i.e., the donor atom becomes more negatively charged and the acceptor atom becomes more positively charged, in contrast to formal atomic charges but in accordance with other calculations on charge transfer in donor−acceptor complexes.[23] Bond angles are only slightly influenced by the Pb−N bond, but the X−Pb−S−C torsion angles (see Table 4) are rather different. For **IIa** and **IIIa** X−Pb−S−C torsion angles are of such a kind that the lone pair of the N atom can favorably interact with the empty valence p-orbital of the Pb atom. An NBO-analysis of **IIIa** and **IIIb** revealed that n_p(S) and n(N) compete for the interaction with the empty valence p-orbital at the Pb atom (see also Ab Initio Conformational Study section further down). For **IIb** and **IIIb**, the anti conformation of the X−Pb−S−C unit allows an optimum π-type n_p(S)−6p(Pb) interaction (see Scheme 2). Exchange of a $SCH_2CH_2NH_2$ group for a Cl atom leads to a significant shortening of the Pb−S and the Pb−N distances. The effect on the

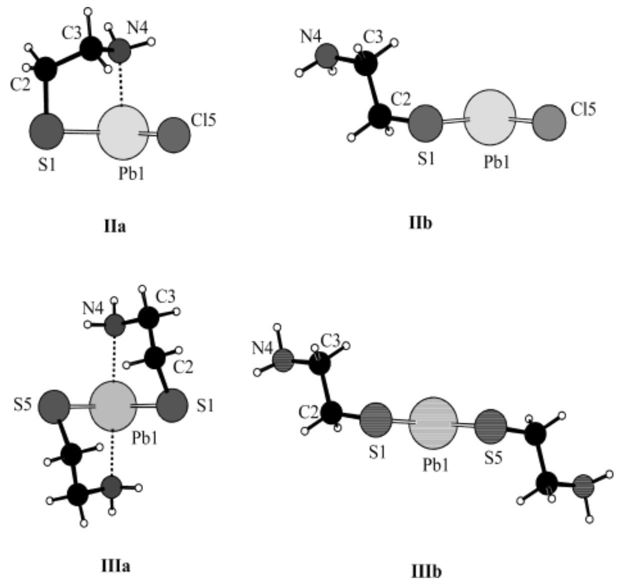

Figure 3. MP2/LANL2DZ(d) optimized structures of conformers **IIa**, **IIb**, **IIIa**, and **IIIb**.

---

(19) Sousa-Pedrares, A.; Casanova, M. I.; Garcia-Vazquez, J. A.; Duran, M. L.; Romero, J.; Sousa, A.; Silver, J.; Titler, P. J. *Eur. J. Inorg. Chem.* **2003**, 678−686.

(20) Peters, K.; Peters, E.-M.; von Schnering, H. G.; Wojnowski, W.; Tamulewicz, S.; Radacki, K. *Z. Kristallogr.-New Cryst. Struct.* **1997**, *212*, 341−342.

(21) The term "conformer" is used according to the definition preferred by Eliel and Wilen, that conformational isomers differ mainly in their torsional angles. Eliel, E. L.; Wilen, S. H. *Stereochemistry of Organic Compounds*; Wiley: New York, 1994.

(22) Reed, A. E.; Curtiss, L. A.; Weinhold, F. *Chem. Rev.* **1988**, *88*, 899−926.

(23) Fleischer, H. *Eur. J. Inorg. Chem.* **2001**, 393−404.

Scheme 2 [a]

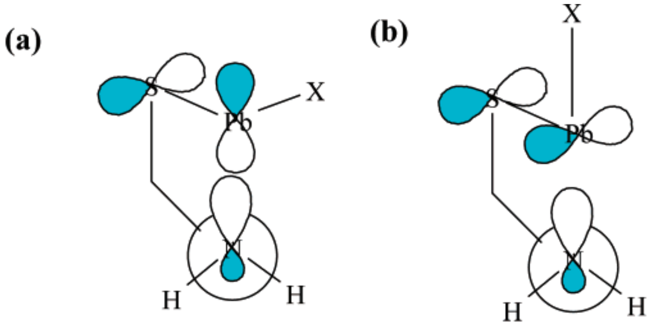

[a] (a) σ-type n(N)−6p(Pb) orbital interaction in **IIa** (X = Cl) and **IIIa** (X = $SCH_2CH_2NH_2$). (b) π-type n_p(S)−6p(Pb) orbital interaction in **IIb** (X = Cl) and in **IIIb** (X = $SCH_2CH_2NH_2$).

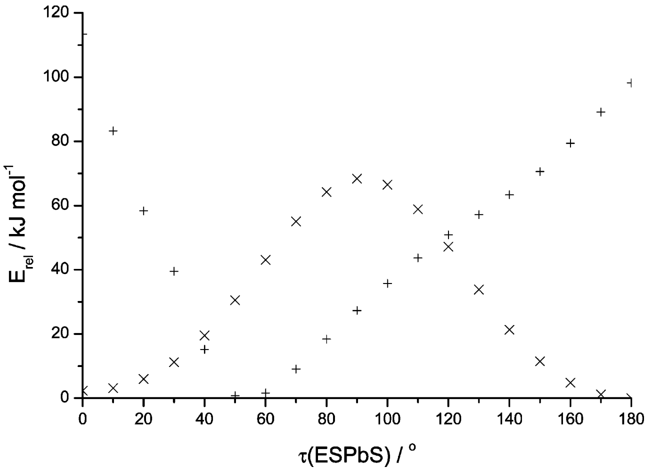

Figure 4. MP2/LANL2DZ(d) potential energy as a function of the SPbSH-torsion of $Pb(SH)_2$ (×) and of the SPbSC-torsion of $Pb(SCH_2CH_2NH_2)_2$ (+).

Pb−S bond is attributed to the fact that the Cl atom is a weaker π-donor than the S atom, since its valence p-type orbitals are of lower energy. Hence, the single S atom can more easily compete with a Cl atom than with another S atom for the empty valence p orbital at the Pb atom. The shorter Pb−N bond in **IIa** compared to that in **IIIa** was already explained in terms of 2c2e- vs 3c4e-bond (vide infra).

A comparison of **IIa** to **2a** reveals the impact of the intermolecular contacts, i.e., hydrogen bridges, Pb1A−S1A#1 and Pb1A−S1B interactions on the molecular structure of $PbCl(SCH_2CH_2NH_2)$; especially the Pb−S and Pb−Cl bonds, which are significantly lengthened by the above-mentioned interactions. A comparison of the ab initio optimized geometry of **IIIa** to the solid-state structure of **3** reveals only small differences in some bond lengths and angles. Pb−S bonds are shorter and Pb···N bonds longer in **IIIa** than in **3**. This observation is attributed to the participation of the S atoms of compound **3** in intermolecular hydrogen bonds, thus leading to weaker Pb−S and hence stronger Pb···N bonds.

Ab Initio Conformational Studies. The model compound $Pb(SH)_2$ (C_2-symmetry), which lacks an N-donor atom in the side chain, was chosen for a scan of the potential energy as a function of the HSPbS torsion parameter (see Figure 4). Two minima were found, with τ(HSPbS) = 0.01° (syn) and 179.98° (anti), respectively, i.e., both structures are close to planar C_{2v}-symmetry. The energy of both forms is rather similar, with the "W" shaped *anti*-conformer being by 2.3 kJ mol^{-1} more stable than the *syn*-conformer. The sum of both π-type n_p(S)−6p(Pb) energies per molecule was calculated as 183 kJ·mol^{-1} and 190 kJ·mol^{-1} for the syn- and the *anti*-conformer, respectively, which are values similar to that obtained for **IIIb** (see Table 4). The structure with τ(HSPbS) = 91.9° represents the transition state between the two minima and its energy is calculated to lay 68.5 kJ mol^{-1} above that of the *anti*-conformer. In contrast, a scan of the CSPbS torsion parameter for $Pb(SCH_2CH_2NH_2)_2$ (C_2-symmetry) revealed a single energy minimum between 0 and 180° which is the one found for **IIIa**. If the torsion angle is lowered or increased, the energy rises, since formation of the stabilizing Pb−N bond becomes increasingly difficult. τ(CSPbS) values close to 0 and 180° represent maxima, instead of minima as was found for $Pb(SH)_2$.

A comparison of the calculations performed for $Pb(SCH_2CH_2NH_2)_2$ to those of $Te(SCH_2CH_2NH_2)_2$ (see ref 9) reveals the impact of different kinds of orbital interactions on molecular conformation. If no E−N interactions were allowed (E = Pb, Te), τ(CSES) took values of 76.2° and 175.7°, for Te and Pb, respectively. In the case of E−N interactions present, τ(CSES) optimized to 135.7° and 53.8°, for Te and Pb, respectively. The differences are due to the orthogonal directions of the acceptor orbitals, σ*(Te−S) (laying in the ES_2 plane) and 6p(Pb) (orthogonal to the ES_2 plane), with which the donor orbitals n_p(S) and n(N) interact and by which interactions the conformations are determined.

Conclusion

2-Aminoethanethiol can form several complexes with Pb^{II}, with the resulting type depending on the kind of lead(II) compound and the stoichiometry of the reactants. In the trinuclear complex $Pb(SCH_2CH_2NH_2)_2$·$2PbCl(SCH_2CH_2NH_2)$ as well as in the mononuclear $Pb(SCH_2CH_2NH_2)_2$, cysteamine chelates the Pb atoms in a bidentate S,N-coordination mode. $PbCl(SCH_2CH_2NH_2)$, a subunit of $Pb(SCH_2CH_2NH_2)_2$·$2PbCl(SCH_2CH_2NH_2)$, is the first structurally characterized PbCl(SR) moiety. Its Pb^{II} atom forms three 2c2e bonds and reaches a formal octet, while in $Pb(SCH_2CH_2NH_2)_2$ a hypervalent Pb^{II} atom is present due to a 3c4e N−Pb−N bond. Ab initio quantum chemical calculations demonstrate that the Pb−N bonds are based on a σ-type n(N)−6p(Pb) interaction, which dominates the π-type n_p(S)−6p(Pb) interaction and hence determines the molecular conformation.

Experimental Section

General Procedures. Lead(II) oxide and lead(II) chloride were purchased from Merck and 2-ammoniumethanethiol chloride was obtained from ACROS. All solvents were purified according to standard procedures; the compounds were handled with Schlenk technique to prevent oxidation of the thiols by air.

Solution NMR: Bruker DRX 400, $B_1(^1H) = 400.0$, $B_1(^{13}C) = 100.577$, $B_1(^{207}Pb) = 83.662$ MHz. Standard: TMS (^1H, ^{13}C) and $PbMe_4$ (^{207}Pb). Solid-state NMR: Bruker DSX 400, $B_1(^{207}Pb) = 83.662$ MHz. Standard: $PbMe_4$. Various magic angle spinning rates between 5000 and 15000 Hz were employed; spectral range scanned

Table 5. Crystal Data for Compounds **2** and **3**[a]

	2	3
empirical formula	$C_{16}H_{24}N_4S_4Cl_2Pb_3$	$C_4H_{12}N_2S_2Pb$
fw/g mol^{-1}	997.02	359.47
cryst syst	monoclinic	orthorhombic
space group	$C2/c$	$Pbca$
Z	4	8
temp/K	193	293
$\rho_{calcd.}$/g cm^{-3}	3.16	2.609
μ/cm^{-1}	24.7[b]	18.82[c]
F(000)	1776	776
cryst size	0.024 × 0.105 × 0.406 mm^3	0.09 × 0.100 × 0.41 mm^3
θ-range	$2.0° < \theta < 28.2°$	$2.1° < \theta < 30.0°$
limiting indices	$-26 \leq h \leq 26, -7 \leq k \leq 7, -23 \leq l \leq 23$	$0 \leq h \leq 13, -26 \leq k \leq 22, -13 \leq l \leq 0$
a/Å	20.0942(15)	9.8426(6)
b/Å	5.8958(4)	19.117(5)
c/Å	17.8169(13)	9.7279(18)
α/deg	90.0	90.0
β/deg	96.9210(12)	90.0
γ/deg	90.0	90.0
V/Å^3	2095.4(5)	1830.4(5)
reflns meas.	9544	3539
unique reflns	2577	2642
refln $\|F\| > 4\sigma(F)$	2240	1431
R $[\|F\| > 4\sigma(F)]$[d]	0.0284	0.0506
GOF on F^2	1.010	0.975
Largest diff. peak and hole	−1.49/1.71 e Å^{-3}	−2.27/2.23 e Å^{-3}

[a] Mo Kα radiation with $\lambda = 0.71069$ Å was used. [b] Absorption correction with MULABS.[30] [c] Absorption correction with psi-scans. [d] $R = \sum ||F_o| - |F_c||/\sum |F_o|$.

from −5000 to +15 000 ppm. IR: Bruker Tensor 27 FTIR, resolution 4 cm^{-1}. The IR spectrum of **2** was recorded in a NaCl matrix and the IR spectrum of **3** was recorded using CsI pellets. IR spectra of **1** were recorded using either NaCl or CsI. UV/vis: JASCO V-570 double beam spectrometer, 190−900 nm, quartz cuvettes, $d = 1$ cm, spectral step width 1 nm, solutions in H_2O of Millipore quality. CHNS analysis was performed with an Elemental Vario EL2.

Preparation of Lead(II) Dichloride (2-ammoniumethanethiolate), $PbCl_2(SCH_2CH_2NH_3)$, 1. A solution of 2-ammoniumethanethiol chloride, $[HSCH_2CH_2NH_3]Cl$, (1.13 g, 10.0 mmol) in 20 mL of 1 M NaOH (20.0 mmol) was added to a stirred suspension of lead(II) chloride, $PbCl_2$, (2.78 g, 10.0 mmol) in 100 mL of ethanol which was heated to reflux. The white solid dissolved to give a pale yellow solution. **1** precipitated from this solution at 5 °C as a yellow solid. Yield: 3.20 g (90.1%). Mp: 230 °C (decomp). Anal. Calcd For $C_2H_7Cl_2NPbS$ (fw = 355.25 g mol^{-1}): C, 6.76; H, 1.99; N, 3.94; S 9.02. Found: C, 6.94; H, 2.00; N, 3.78; S, 8.97. IR: (NaCl pellet, 4000−500 cm^{-1}): 3446 (br, vs, ν(N−H)), 3066 (br, vs, ν(N−H)), 2922 (s, $\nu(CH_2)$), 2856 (sh, $\nu(CH_2)$), 1650 (s, δ(N−H)), 1574 (s, δ(N−H)), 1567 (s, δ(N−H)), 1481 (vs, $\delta(CH_2)$), 1459 (sh, $\delta(CH_2)$), 1371 (w, $\delta(CH_2)$), 1313 (w), 1254 (m), 1124 (s), 1057 (m), 921 (m), 876 (w), 801 (w), 756 (m).

Preparation of Lead(II) Bis(2-aminoethanethiolate)−Lead(II) (2-aminoethanethiolate) Chloride (1/2), $Pb(SCH_2CH_2NH_2)_2 \cdot 2PbCl(SCH_2CH_2NH_2)$, 2. A solution of $[HSCH_2CH_2NH_3]Cl$ (2.27 g, 20.0 mmol) in 70 mL of 1 M NaOH (70 mmol) was added to a refluxed and stirred suspension of $PbCl_2$ (2.78 g, 10.0 mmol) in 100 mL of ethanol. The white solid dissolved to give a pale yellow solution which lost its color during 24 h of heating under reflux. On cooling to 5 °C, the product precipitated as colorless crystals. Yield: 3.08 g (92.7%). A single crystal of **2** suitable for X-ray diffraction was obtained from the precipitate. Mp: 150 °C (decomp). Anal. Calcd For $C_8H_{24}Cl_2N_4Pb_3S_4$ (fw = 997.02 g mol^{-1}): C, 9.63; H, 2.43; N, 5.62; S 12.86. Found: C, 9.57; H, 2.46; N, 5.58; S, 12.84. IR (NaCl pellet, 4000−500 cm^{-1}) 3291 (m, ν(N−H)), 3238 (m, ν(N−H)), 3163 (w, ν(N−H)), 3143 (m, ν(N−H)), 3080 (m, ν(N−H)), 2933 (m, $\nu(CH_2)$), 2907 (m, $\nu(CH_2)$), 2891 (m, $\nu(CH_2)$), 2848 (m, $\nu(CH_2)$), 1582 (s, $\delta(NH_2)$), 1568 (sh, $\delta(NH_2)$), 1441 (m, $\delta(CH_2)$), 1419 (m, $\nu(CH_2)$), 1372 (w, $\delta(CH_2)$), 1285 (s, $\delta(CH_2)$), 1260 (s, $\delta(CH_2)$), 1230 (w, $\delta(CH_2)$), 1216 (w, $\delta(CH_2)$), 1031 (vs, ν(N−C)), 970 (m), 941 (s), 913 (s), 835 (s, ν(S−C)), 656 (s, ν(S−C)), 601 (m, ν(S−C)), 559 (m, δ(S−C)). UV/vis: $c = 1.23\ 10^{-5}$ M ($\lambda_{max} = 202$ nm, $\epsilon(\lambda_{max}) = 5.4\ 10^4$ L mol^{-1} cm^{-1}; $\lambda_{max} = 272$ nm, $\epsilon(\lambda_{max}) = 0.9\ 10^4$ L mol^{-1} cm^{-1}).

Preparation of Lead(II) Bis(2-aminoethanethiolate), $Pb(SCH_2CH_2NH_2)_2$, 3. $[HSCH_2CH_2NH_3]Cl$ (2.84 g, 25.0 mmol) dissolved in 25 mL of 1 M NaOH (25 mmol) was added to a stirred suspension of PbO (2.78 g, 10.0 mmol) in 100 mL of ethanol kept at 50 °C. The yellow solid dissolved to give a pale yellow solution which was refluxed for 3 h. A small amount of a gray precipitate was removed by filtration and the filtrate was kept at 5 °C. From this solution, **3** precipitated as colorless crystals. Yield: 2.98 g (82.9%). A single crystal of **3** suitable for X-ray diffraction was obtained from the precipitate. Mp: 110 °C. Anal. Calcd for $C_4H_{12}N_2PbS_2$ (fw = 359.47 g mol^{-1}): C, 13.36; H, 3.36; N, 7.79; S 17.84. Found: C, 13.45; H, 3.41; N, 7.75; S, 17.77. ^{1}H NMR (D_2O): 2.800 (t, ^3J(H,H) = 6.0 Hz, 2H, NCH_2), 2.683 (t, ^3J(H,H) = 6.1 Hz, 2H, SCH_2), signal of NH_2 was not observed. IR (CsI pellet, 4000−200 cm^{-1}): 3363 (vs), 3294(vs), 3240(vs) and 3084(s), all ν(N−H); 2944, 2932, 2911, 2890 and 2848, all (m, $\nu(CH_2)$); 1586(s) and 1560(m), all $\delta(NH_2)$; 1449 (vs), 1290(m), 1262(m) and 1232(m), all $\delta(CH_2)$; 1046 and 1032, all (s, ν(N−C)); 944(s), 914(s), 866(m, ν(S−C)), 839(m, ν(S−C)), 465(s, $\rho(NH_2)$), 343(vs). UV/vis: $c = 4.00\ 10^{-5}$ M ($\lambda_{max} = 201$ nm, $\epsilon(\lambda_{max}) = 2.0\ 10^4$ L mol^{-1} cm^{-1}; λ_{max} 270 nm, $\epsilon(\lambda_{max}) = 0.3\ 10^4$ L mol^{-1} cm^{-1}).

Crystal Structure Determination. Diffraction experiments were performed on a BRUKER Nonius CCD diffractometer. The crystal structures were solved by direct methods and difference Fourier technique (SIR-92),[24] and structural refinement was against F^2

---

(24) Altomare, A.; Cascarano, G.; Giacovazzo, C.; Guagliardi, A.; Burla, M. C.; Polidori, G.; Camalli, M.: *SIR − A Program for the Automatic Solution of Crystal Structures by Direct Methods. J. Appl. Crystallogr.* **1994**, *27*, 435−436.

(SHELXL-97).[25] Details of the crystal structure determination of compounds **2** and **3** and their crystal data are given in Table 5.

Theoretical Methods. The ab initio calculations were performed on various personal computers using the GAUSSIAN94 and GAUSSIAN98 software packages.[26,27] Geometry optimization and calculation of vibrational frequencies were performed at the Hartree−Fock level (HF), followed by second-order Møller Plesset perturbation theory (MP2), with an effective core double-ζ valence basis set according to Hay and Wadt[28] augmented by appropriate polarization functions for Pb, S (with exponents according to Höllwarth et al.[29]), N (exponent 0.80), and C (exponent 0.75), and the basis set being designated as LANL2DZ(d). To create suitable starting geometries, standard interatomic distances and bond angles were used. To distinguish between conformational isomers, appropriate starting values for the C−S−Pb−S torsion angle were used. Only MP2/LANL2DZ(d) structures and thermochemical data, are presented. At the MP2/LANL2DZ(d) level an analysis of the electronic structure in terms of natural orbitals was also performed.[22]

Acknowledgment. We thank the Johannes Gutenberg-Universität Mainz and the Fonds der Chemischen Industrie for financial support.

Supporting Information Available: X-ray crystallographic files in CIF format for all structures presented. This material is available free of charge via the Internet at http://pubs.acs.org.

IC0498889

---

(25) Sheldrick, G. M. SHELXL-97 *Program for Crystal Structure Refinement*, Universität Göttingen, Germany, 1997.

(26) Frisch, M. J.; Trucks, G. W.; Schlegel, H. B.; Gill, P. M. W.; Johnson, B. G.; Robb, M. A.; Cheeseman, J. R.; Keith, T.; Petersson, G. A.; Montgomery, J. A.; Raghavachari, K.; Al-Laham, M. A.; Zakrzewski, V. G.; Ortiz, J. V.; Foresman, J. B.; Cioslowski, J.; Stefanov, B. B.; Nanayakkara, A.; Challacombe, M.; Peng, C. Y.; Ayala, P. Y.; Chen, W.; Wong, M. W.; Andres, J. L.; Replogle, E. S.; Gomperts, R.; Martin, R. L.; Fox, D. J.; Binkley, J. S.; Defrees, D. J.; Baker, J.; Stewart, J. P.; Head-Gordon, M.; Gonzalez, C.; Pople, J. A. *Gaussian 94, Revision E.2*; Gaussian, Inc.: Pittsburgh, PA, 1995.

(27) Frisch, M. J.; Trucks, G. W.; Schlegel, H. B.; Scuseria, G. E.; Robb, M. A.; Cheeseman, J. R.; Zakrzewski, V. G.; Montgomery, Jr., J. A.; Stratmann, R. E.; Burant, J. C.; Dapprich, S.; Millam, J. M.; Daniels, A. D.; Kudin, K. N.; Strain, M. C.; Farkas, O.; Tomasi, J.; Barone, V.; Cossi, M.; Cammi, R.; Mennucci, B.; Pomelli, C.; Adamo, C.; Clifford, S.; Ochterski, J.; Petersson, G. A.; Ayala, P. Y.; Cui, Q.; Morokuma, K.; Malick, D. K.; Rabuck, A. D.; Raghavachari, K.; Foresman, J. B.; Cioslowski, J.; Ortiz, J. V.; Stefanov, B. B.; Liu, G.; Liashenko, A.; Piskorz, P.; Komaromi, I.; Gomperts, R.; Martin, R. L.; Fox, D. J.; Keith, T.; Al-Laham, M. A.; Peng, C. Y.; Nanayakkara, A.; Gonzalez, C.; Challacombe, M.; Gill, P. M. W.; Johnson, B.; Chen, W.; Wong, M. W.; Andres, J. L.;. Gonzalez, C.; Head-Gordon, M.; Replogle, E. S.; Pople, J. A. *Gaussian 98, Revision A.6*; Gaussian, Inc.: Pittsburgh, PA, 1998.

(28) Wadt, W. R.; Hay, P. J. *J. Chem. Phys*. **1985**, *82*, 284−298.

(29) Höllwarth, A.; Böhme, M.; Dapprich, S.; Ehlers, A. W.; Gobbi, A.; Jonas, V.; Köhler, K. F.; Stegmann, R.; Veldkamp, A.; Frenking, G. *Chem. Phys. Lett*. **1993**, *208*, 237−240.

(30) Blessing, R. *Acta Crystallogr*. **1995**, *A51*, 33−38.